Geophysical Research Letters

RESEARCH LETTER
10.1002/2017GL076268

Relations Between v_z and B_x Components in Solar Wind and their Effect on Substorm Onset

Marina Kubyshkina[1], Vladimir Semenov[1], Nikolay Erkaev[2,3], Evgeny Gordeev[1], Stepan Dubyagin[4], Natalia Ganushkina[4,5], and Maria Shukhtina[1]

[1]Earth Physics Department, Saint Petersburg State University, Saint Petersburg, Russia, [2]Institute of Computational Modelling, Federal Research Center "Krasnoyarsk Science Center SB RAS", Akademgorodok, Russia, [3]Department of Applied Mechanics, Siberian Federal University, Krasnoyarsk, Russia, [4]Finnish Meteorological Institute, Helsinki, Finland, [5]Department of Climate and Space Sciences and Engineering, University of Michigan, Ann Arbor, MI, USA

Key Points:
- Using two substorm lists, we show that for two thirds of all substorm onsets, the ($B_x \cdot v_z$) product in the solar wind has the same sign as the IMF B_z
- When the signs of the product ($B_x \cdot v_z$) and the IMF B_z coincide, the asymmetry (bending) of the magnetotail current sheet increases
- Signs correlation of ($B_x \cdot v_z$) and B_z in the SW (a feature of Alfvénic waves propagating from the Sun) is observed during two thirds of all the time

Correspondence to:
M. Kubyshkina,
m.kubyshkina@spbu.ru

Citation:
Kubyshkina, M., Semenov, V., Erkaev, N., Gordeev, E., Dubyagin, S., Ganushkina, N., & Shukhtina, M. (2018). Relations between v_z and B_x components in solar wind and their effect on substorm onset. *Geophysical Research Letters*, *45*, 3760–3767. https://doi.org/10.1002/2017GL076268

Received 2 NOV 2017
Accepted 16 MAR 2018
Accepted article online 26 MAR 2018
Published online 4 MAY 2018

Abstract We analyze two substorm onset lists, produced by different methods, and show that the ($B_x \cdot v_z$) product of the solar wind (SW) velocity and interplanetary magnetic field (IMF) components for two thirds of all substorm onsets has the same sign as IMF B_z. The explanation we suggest is the efficient displacement of the magnetospheric plasma sheet due to IMF B_x and SW flow v_z, which both force the plasma sheet moving in one direction if the sign of ($B_x \cdot v_z$) correlates with the sign B_z. The displacement of the current sheet, in its turn, increases the asymmetry of the magnetotail and can alter the threshold of substorm instabilities. We study the SW and IMF data for the 15-year period (which comprises two substorm lists periods and the whole solar cycle) and reveal the similar asymmetry in the SW, so that the sign of ($B_x \cdot v_z$) coincides with the sign of IMF B_z during about two thirds of all the time. This disproportion can be explained if we admit that about 66% of IMF B_z component is transported to the Earth's orbit by the Alfvén waves with antisunward velocities.

Plain Language Summary We explore the interplanetary magnetic field configuration together with the direction of the solar wind flow velocity to demonstrate that the plasma sheet motion, which is caused by both magnetic field component B_x and solar wind flow component v_z, may affect the substorm onset. The obtained statistical result shows that the number of substorms, which broke in a situation when IMF Bz has the same sign as ($B_x \cdot v_z$) (favorable for the plasma sheet displacement), is 30–50% larger than the number of other substorms. The same relation was obtained for two different substorm onset databases, one obtained from Imager For Magnetopause-to-Aurora Global Exploration Far Ultraviolet observations and the other from ground-based AL index.

1. Introduction

It is commonly accepted now that the existence of a southward component of interplanetary magnetic field (IMF) is the main driver of magnetospheric activity (Akasofu, 1975; Fairfield & Cahill, 1966; Rostoker & Falthammar, 1967), since the southward direction of IMF is favorable for the magnetic reconnection at the magnetopause (Dungey, 1961). Yet the questions on when, why, and how does the substorm expansion develop are still under discussion. One of the possible reasons for this long-lasting discussion is the great variability of substorms behavior and substorm onset configurations (see, for example, recent paper by Borovsky and Yakymenko (2017), and references therein.) One of the important problems in this context is the existence of an external driver for substorm triggering. Recent study by Newell et al. (2016) demonstrated a clear dependence of substorm probability on the solar wind (SW) speed and claimed that the SW speed is the main predictor for substorm occurrence. That study also showed that any change in IMF B_z or SW speed increases the odds of a substorm if compared to no change, and, especially, if it is a drop in SW speed or a northward turn in IMF B_z. Both of these factors slow down the rate of the magnetic field merging on the dayside magnetopause, but they do not significantly change the geometry of the magnetospheric configuration.

Our study stays somewhat aside from the mainstream of substorm research; we explore the SW flow v_z component and the IMF B_x component as the factors that change the rate of the asymmetry of magnetospheric configuration (see, for example, (Hoilijoki et al., 2014; Sergeev et al., 2008; Tsyganenko & Fairfield, 2004)) and analyze how do they vary when approaching a substorm onset.

At present, there exist a few studies (Kubyshkina et al., 2015; Panov et al., 2012; Semenov et al., 2015; Vörös et al., 2014) that explore the substorm behavior in a situation with changing SW flow velocity. They show that fast changes in the SW flow v_z component, especially in a situation with nonzero dipole tilt, may facilitate a substorm onset. A reason for that may be an additional curving and displacement of magnetospheric plasma sheet that lowers the substorm instability threshold in an asymmetric bent current sheet (e.g., Kivelson & Hughes, 1990).

However, the v_z component of the flow velocity is not the only SW parameter that causes plasma sheet motion in the vertical (normal to ecliptic plane) direction. The existence of a nonzero B_x component of IMF results in a displacement of an X-line for the dayside magnetopause reconnection and in the asymmetric magnetic flux circulation in magnetospheric lobes (Cowley, 1981; Gordeev et al., 2016; Reistad et al., 2014). Magnetic flux imbalance in the northern and southern lobes leads, in turn, to the plasma sheet displacement from its equilibrium position. Depending on the sign of the B_x, the plasma sheet will move up or down in a similar way as it does due to a nonzero v_z component of the SW flow.

Therefore, in the present paper, we investigate the mutual effect of both the SW flow v_z component and the IMF B_x component on substorm probability. In section 2 we describe the details of motivation of this study, in section 3 we study the presubstorm statistics, in section 4 we examine the SW and IMF data, and, finally, in section 5 we put together the results and discuss them.

2. Motivation Details and Background

The existence of the negative IMF B_z (here and below in this section we use Geocentric Solar Magnetic coordinates) is one of the key requirements for a magnetospheric substorm initiation. Yet it is also clear that there exist other factors that force or slow down the substorm onset and vary the amount of energy stored during the growth phase and released during the expansion phase.

If, based on previous works (Kivelson & Hughes, 1990; Kubyshkina et al., 2015; Panov et al., 2012; Semenov et al., 2015), we admit that the increased asymmetry of the magnetotail configuration lowers the threshold for substorm triggering instability, we need to check how do the SW v_z component and the IMF B_x component change the position of the magnetospheric plasma sheet.

Following the direction of the SW plasma flow, the magnetospheric plasma sheet will move up from the ecliptic plane under positive SW flow velocity component v_z and down under negative v_z, irrespective of the sign of the IMF B_z.

The displacement of the plasma sheet under the nonzero IMF B_x is caused by the nonsymmetric dayside reconnection, when the X-line is shifted from the subsolar point. As a result, the unbalanced reconnected magnetic fluxes in the southern and northern magnetotail lobes force the plasma sheet moving up or down from the ecliptic plane (see Cowley, 1981; Gordeev et al., 2016; Reistad et al., 2014). The rate of this displacement will be large only under negative IMF B_z, when the dayside reconnection is active. This phenomenon is illustrated in Figure 1, adopted from Cowley (1981). Under negative IMF B_z, the plasma sheet will move down with positive B_x component, and plasma sheet will move up the equatorial plane with the negative B_x component.

After we compare the plasma sheet reaction to the nonradial SW plasma flow and nonzero IMF B_x, we see that when IMF B_z is negative, the plasma sheet moves up with $B_x < 0$ and with $v_z > 0$, and the plasma sheet goes down with $B_x > 0$ and with $v_z < 0$. Thus, the rate and velocity of plasma sheet displacement will be maximal if the sign of a product $(v_z \cdot B_x)$ is the same as the sign of the B_z.

If the substorm onset happens under positive IMF B_z, usually it means that the IMF B_z changes its sign from negative to positive in a late growth phase. In this case, when the IMF B_z turns northward, the dayside reconnection stops and the previously (during the period with negative B_z) shifted plasma sheet starts to move in the opposite direction (up for B_x positive and down for B_x negative). Thus, the current sheet displacement due to the existence of the nonzero B_x and v_z will maximize if $(v_z \cdot B_x) > 0$, that is, again , has the same sign as IMF B_z.

If we assume that the displacement of the plasma sheet is a favorable factor for a substorm onset, we would expect that a number of substorms, which start under the IMF B_z and $(v_z \cdot B_x)$ with the same signs, should be larger than the number of substorms that starts when the signs of the B_z and $(v_z \cdot B_x)$ are opposite.

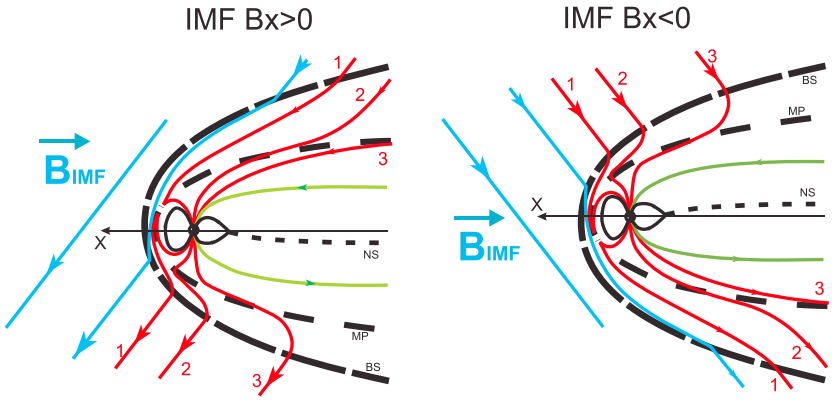

Figure 1. The directions of plasma sheet motion in the presence of positive (left) and negative (right) IMF B_x component for southward IMF B_z. The blue lines correspond to IMF lines, the red lines are the reconnected magnetospheric-IMF lines, and the green lines are Earth's magnetotail field lines. The thick black dashed lines mark the position of bow shock (BS), magnetopause (MP), and neutral sheet (NS). IMF = interplanetary magnetic field.

3. Data Analysis: Substorm Activity

To verify the above suggestion, we used the two principally different substorm databases:

1. the list of substorms from Frey et al. (2004), which is based on Far Ultraviolet data from Imager for Magnetopause-to-Aurora Global Exploration satellite and contains 4,193 substorm onsets during 2000 to 2005, and
2. the list of substorms from SuperMAG ground-based magnetic observations (http://supermag. jhuapl.edu/substorms/) based on automatic analysis of AL index behavior that contains 18,807 substorm onsets during 2000–2010, the period that comprises the period of the Frey et al. (2004) data list and also includes both minimum and maximum of the solar cycle activity.

Each database was complemented with OMNI data, containing 5-min values of IMF and SW flow velocity for 1 hr preceding the substorm onsets. After that, all the substorms were divided into two groups: those that started during southward B_z ($B_z < -1$ nT) and those that began under northward B_z ($B_z > 1$ nT). We used only those onsets, where OMNI data (for both magnetic field and solar flow) was available at the onset time. We excluded the near-zero values of B_z to avoid possible uncertainties, since the sign of B_z is crucial for our analysis. For Frey et al. (2004) data the number of exclusions with $-1 < B_z < 1$was equal to 880 onsets (out of 3,989 that had the OMNI data), and for SuperMAG data set we had 2,966 exclusions (out of 18,114 onsets with the OMNI data).

The resulting distributions of a number of substorms with different $(v_z \cdot B_x)$ values at the time of a substorm onset (5-min averaged values which precede 5-minutes period, containing a substorm onset) are given in Figure 2 for both lists of substorms and in two types of histograms: the two-column histogram gives the numbers of substorms with all positive and all negative occurrences of $(v_z \cdot B_x)$, and the 20-column histogram shows a more detailed distribution.

Figure 2a shows the discussed distributions only for the substorms, which started under negative IMF B_z, with two histograms on the left for Frey et al. (2004) substorm list and two histograms on the right for SuperMAG substorm list. Both substorm lists give the same imbalance in the number of substorms with different signs of $(v_z \cdot B_x)$, the number of substorms that started under negative $(v_z \cdot B_x)$ is almost twice (1.75 times) larger than the number of substorms that started under positive $(v_z \cdot B_x)$ (see two-column histograms in Figure 2a). Also, it is important to note that this difference is well reproduced in each pair of bins (positive and negative) of 20-column histograms and becomes even larger for the larger values of $(v_z \cdot B_x)$ (see Figure 2a).

Figure 2b gives the same histograms for the substorms with the onsets under positive IMF B_z ($B_z > 1$ nT). The total number of these substorms is much smaller, their intensity is small on average, but the distributions are very similar, with almost twice average of substorms that started under positive values of $(v_z \cdot B_x)$ (see two-column histograms in Figure 2b) and with more notable differences in substorm numbers for larger values of $(v_z \cdot B_x)$ (see 20-column histograms in Figure 2b).

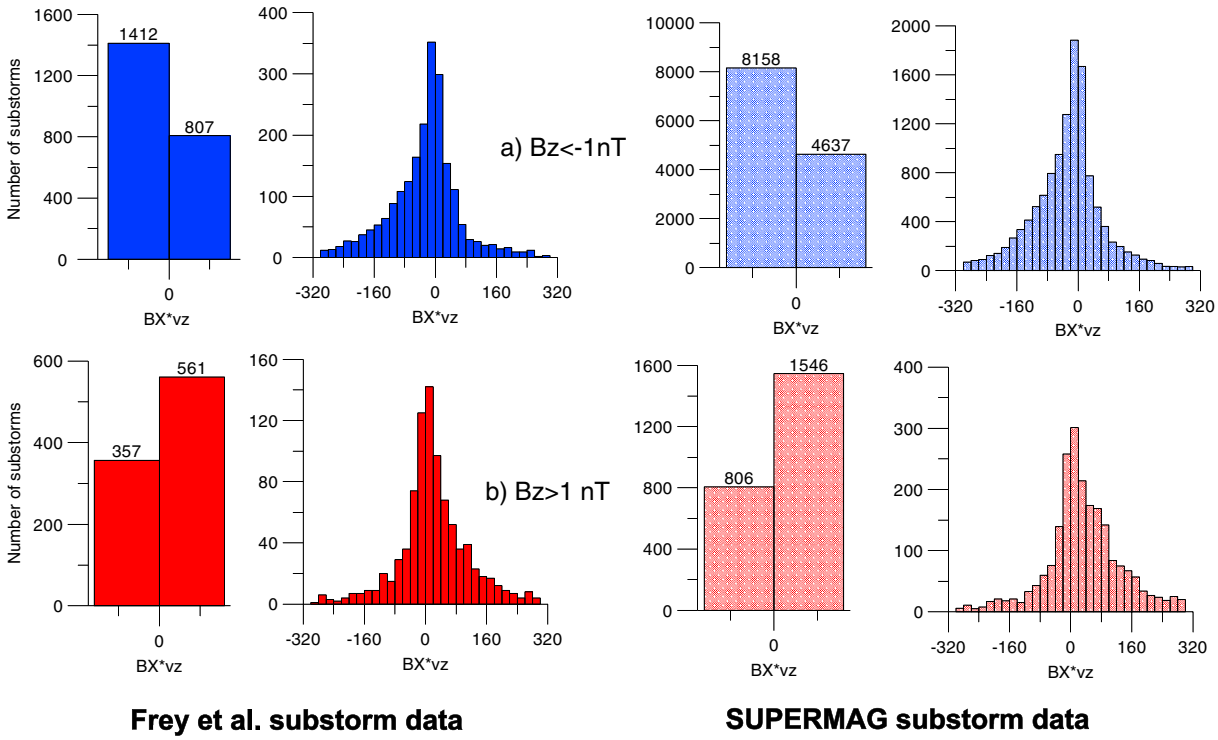

Figure 2. Histograms for the number of substorms with different values of $(v_z \cdot B_x)$, measured near the time of a substorm onset, for two substorm lists (on the right and on the left) and for (a and b) both signs of IMF B_z.

The next important question is if the distribution that we observe near a moment of a substorm onset remains unchanged throughout the growth phase? To check it, we made the time series of 12 two-column histograms for both lists of substorms (the same as those in Figure 2) for twelve 5-min averaged points before the onset (for simplicity we used the same 1-hr period as a growth phase for all the substorms). Using those histograms, we tracked how the relative number of the events for which $(v_z \cdot B_x)$ is positive/negative changes during the growth phase (or more precisely, during 1 hr before the substorm onset). The results are given in Figure 3. Each point on this plot is obtained as a relative difference (in percent) between the number of the events when $(v_z \cdot B_x)$ was negative at a given time before onset and the number of the events when $(v_z \cdot B_x)$ was positive at the same time (i.e., the difference between two bins in the two-column histograms), normalized by the total number of substorms under the given sign of IMF B_z. Blue lines are used for the substorms that start under ($B_z < -1$ nT), and red lines are for the substorms with the onsets under ($B_z > 1$ nT), the points from SuperMAG database are marked by crosses and the points for Frey et al. (2004) substorm database are marked by triangles. Substorm onset is marked by zero on the horizontal axis. We see that the difference between the number of events where the sign of $(v_z \cdot B_x)$ coincides with the sign of B_z increases before a substorm onset and maximizes close to an onset (note that we use 5-min averages for B_x and v_z). From Figure 3 one can also see that for both databases, the lines look quite similar, they start at less than 5% difference at the beginning of the growth phase (or, more precisely, 1 hr before an onset) and reach almost the same maximal value of about 30%, which means almost twofold difference between the number of substorms with the same sign of B_z and $(v_z \cdot B_x)$ and the number of substorms with the opposite signs of those. At the same time, there is a certain distinction in the behavior of red and blue lines (for positive and negative B_z); while the blue lines show a gradual increase during the whole period of 1 hr with a more steep rise in last 10 min, the red lines remain at approximately the same values during first 30–40 min of a growth phase and then steeply go down in the last 20 min before a substorm onset, change sign, and reach maximum close to an onset.

The above statistics allows one to conclude that two thirds of magnetospheric substorms start under the situation when magnetotail plasma sheet moves in the same direction (up or down the ecliptic plane) due to both IMF B_x and solar wind v_z, and since the number of periods with correlated signs of B_z and $(v_z \cdot B_x)$ increases notably before the substorm onset, it is reasonable to admit that this sign correlation (which increases the asymmetry of the magnetotail) can facilitate a substorm onset.

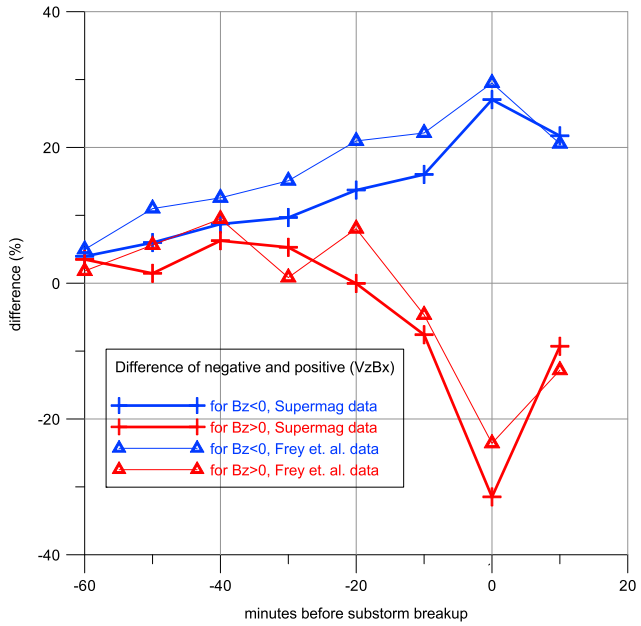

Figure 3. Time dependence of the difference between the number of the events when $(v_z \cdot B_x)$ was negative at a given time before onset, and the number of events when $(v_z \cdot B_x)$ was positive at the same time. Blue lines correspond to the substorm onsets under negative B_z, red lines to those under positive B_z, lines with triangles show Frey et al. database, and lines with crosses show SuperMAG database.

Here it is important to compare our results with a traditional idea of substorm triggering by northward IMF B_z turning (Lyons et al., 1997), which has been strongly criticized in the last 10 years (see Freeman & Morley, 2009; Morley & Freeman, 2007; Newell et al., 2016). The results of superposed epoch analysis for the IMF B_z are presented in Figure 4 separately for two groups of substorms: those with the same sign of IMF B_z and $(v_z \cdot B_x)$ before onset, and those with the opposite signs of IMF B_z and $(v_z \cdot B_x)$. The solid line in Figure 4 corresponds to all the events that have IMF $B_z < -1$ nT and $(v_z \cdot B_x) < 0$ together with the events where IMF $B_z > 1$ nT and $(v_z \cdot B_x) > 0$. The dashed line comprises the other two groups of substorms. The analysis is done for SuperMAG data set (Figure 4, left) and for Frey et al. (2004) data set (Figure 4, right), with similar results. Both plots show the IMF B_z turning northward, and thus, the substorm triggering by northward INF B_z turning is supported by our analysis. Also, both plots show smaller mean IMF B_z for the same sign substorms, given by solid lines. The smaller IMF B_z throughout the whole growth phase confirms our suggestions that these substorms start in average after lower energy input and thus would have lower substorm instability threshold.

4. $(v_z \cdot B_x)$ Distribution in the SW

After we obtained the above sign correlations of B_z and $(v_z \cdot B_x)$ near a substorm onset, it is important to verify if the same correlation is a regular feature in the SW. For consistency, we analyzed the OMNI data for the similar (slightly widened) period, that is, for the years 1996–2011. For the SW and the IMF components, we used the Geocentric Solar Ecliptic (GSE) frame, relevant for the SW studies. Again, for consistency, we used 5-min averages. For each year in this period (1996–2011) we analyzed the distributions of $(v_z \cdot B_x)$ for both positive ($B_z > 1$ nT) and negative ($B_z < -1$ nT) signs of IMF B_z. For all the 5-min periods during the given year when the IMF B_z was negative (< -1 nT) we calculated the number of 5-min periods when $(v_z \cdot B_x)$ was negative and the number of 5-min periods when it was positive. The difference between these numbers (in percent) normalized by the whole number of 5-min periods when IMF B_z was less than -1 nT, calculated for each year (a measure similar to that in section 3), is plotted in Figure 5 with the blue line. After that, the same procedure was performed for the periods when the IMF B_z was positive (> 1 nT). The red line in Figure 5 shows the same relative difference, calculated for the periods, with IMF $B_z > 1$ nT. The Wolf numbers are given in black for reference.

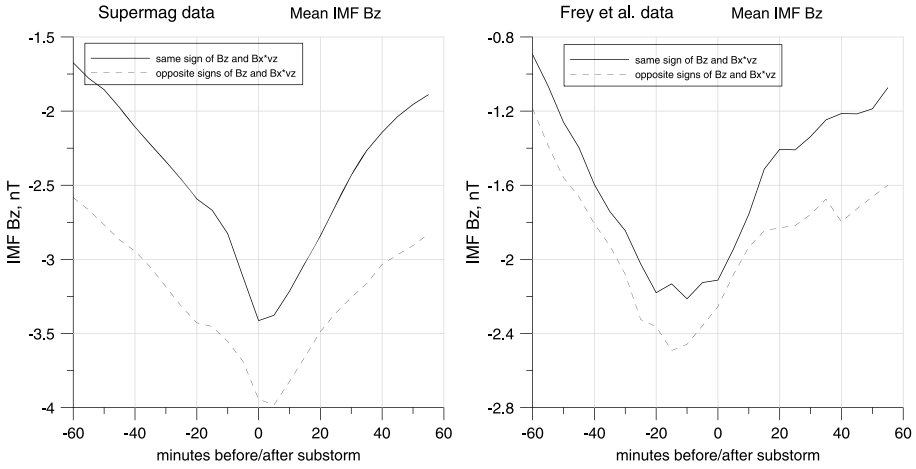

Figure 4. IMF B_z superposed epoch analysis for 2 different substorm classes, which are defined by the signs of IMF B_z and $(v_z \cdot B_x)$ near the onset. Solid lines correspond to the ensemble means of substorms which started under the same sign of B_z and $(v_z \cdot B_x)$, dashed lines - to those, which started under opposite B_z and $(v_z \cdot B_x)$

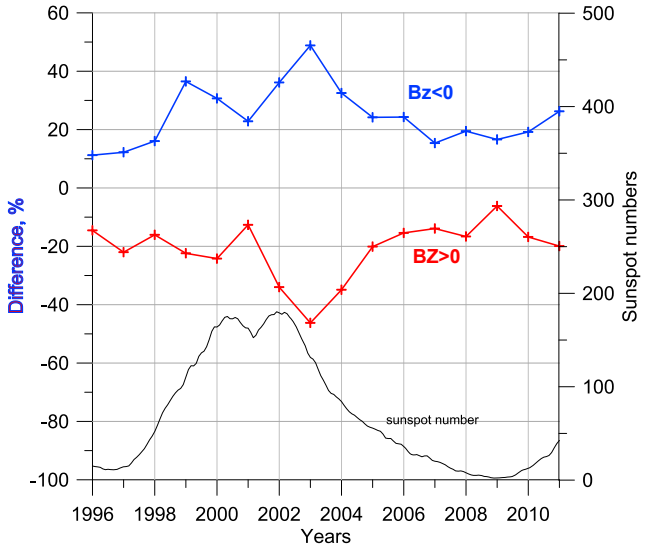

Figure 5. The normalized annual difference between the number of 5-min periods with negative and positive $(v_z \cdot B_x)$ (in percent), calculated for the times when IMF B_z was less than −1 nT (blue line) or IMF B_z was greater than +1 nT (red line). The black line gives the sunspot numbers.

The resulting Figure 5 demonstrates the same type of imbalance as was obtained in section 3. The values from the blue line are always positive; the red line gives only negative values (i.e., the number of periods with the same signs of the IMF B_z and $(v_z \cdot B_x)$ is always greater than the number of periods with the opposite signs of those). In other words, the sign of the $(v_z \cdot B_x)$ follows more often the sign of IMF B_z, rather than has the opposite sign. The degree of this imbalance varies with the solar cycle, and it reaches maximal values (almost 50%, which means 3 times excess) soon after the solar maximum and becomes much smaller (about 10–15%) at solar minimum. It is interesting to note that a very similar behavior of the substorm occurrence rates throughout a solar cycle was reported in Tanskanen (2009).

5. Discussion and Conclusions

Our analysis showed that almost twice larger number of substorms onsets are observed in the periods when the IMF and SW parameters B_z and $(v_z \cdot B_x)$ have the same signs, if compared to the periods when those signs are opposite. These are the periods when the magnetotail plasma sheet is forced to move in the same direction (up or down from the ecliptic plane) due to both the SW flow velocity and the IMF B_x component. We also showed that the difference between the number of events with positive and negative values of $(v_z \cdot B_x)$ increases during the period of a growth phase, which may be interpreted as additional trigger for a substorm onset. Indeed, if the number of occurrences of $(v_z \cdot B_x)$ with a proper sign (the same as the IMF B_z has) increases closer to an onset, it means that either v_z or B_x changes sign, which results in the enhancing of the plasma sheet displacement.

The statistical analysis of SW v_z and IMF B_x and B_z, provided in this study, shows that in the SW, also, the sign of the $(v_z \cdot B_x)$ follows more often the sign of IMF B_z, rather than has the opposite one.

A simple interpretation of these results implies that the imbalance in the number of periods with different signs of $(v_z \cdot B_x)$ is produced due to the Alfv́en-type disturbances, propagating from the Sun. The importance and geo-effectiveness of Alfv́en waves was discussed in a great number of papers, see Belcher and Davis (1971), Snekvik et al. (2013), and Zhang et al. (2014), and references therein. Indeed, if we assume that the undisturbed SW flows radially with V_{0x} velocity in the Sun-Earth direction (i.e., along the X_{GSE} axis) and that the IMF background component is also radial and equal to B_{0x}, then, for a plane Alfvén-type wave disturbances (**b** and **v**) propagating along the Sun-Earth line (along the X_{GSE} axis)

$$\mathbf{b} = \mathbf{b}(x + ut) \quad \text{and} \quad \mathbf{v} = \mathbf{v}(x + ut)\ . \tag{1}$$

Here u is the wave velocity in a fixed frame of reference related to Earth, so that

$$u = \pm v_A + |V_{0x}|, \tag{2}$$

where v_A is the Alfvén velocity, and signs "+" and "−" correspond to antisunward and sunward directions, respectively. The linearized equation of motion then will look like (for Alfvén-type wave we also put total pressure gradient equal to zero: $\nabla P = 0$) :

$$\rho \cdot \left(\frac{\partial \mathbf{v}}{\partial t} + V_{0x}\frac{\partial \mathbf{v}}{\partial x}\right) = \frac{1}{4\pi} \cdot \left(B_{0x}\frac{\partial \mathbf{b}}{\partial x}\right)\ . \tag{3}$$

where ρ is the plasma mass density. Note that V_{0x} here is negative, so $V_{0x} = -|V_{0x}|$. Using (2), we substitute (1) to equation (3) and get

$$\rho\left(\frac{\partial \mathbf{v}}{\partial x}\right) = \pm\frac{1}{4\pi v_A} \cdot B_{0x}\left(\frac{\partial \mathbf{b}}{\partial x}\right)\ . \tag{4}$$

Equation (4) yields the following relationship between the velocity and magnetic field perturbations

$$\rho \cdot \mathbf{v} = \pm \frac{1}{4\pi v_A} \cdot B_{0x} \cdot \mathbf{b} \,, \tag{5}$$

or, for the z components (and after multiplying by B_{0x})

$$\rho \cdot (v_z \cdot B_{0x}) = \pm \frac{1}{4\pi v_A} \cdot B_{0x}^2 \cdot b_z \,. \tag{6}$$

From the equation (6) one can see that in the case of earthward (antisunward) propagating waves the product $(v_z \cdot B_{0x})$ has the same sign as b_z component.

If the Alfvén-type disturbances are born away from the Sun, we expect to observe two waves: directed to and from the Sun. If the disturbances appear near the Sun, where the plasma flow velocities are smaller than the Alfvén velocity, we will observe only one wave, directed earthward. Thus, the excess number of periods with correlated signs of the IMF B_z and $(v_z \cdot B_x)$, reported in section 4, probably, corresponds to the near-Sun-born disturbances. Since the more active Sun produces larger amount of Alfvén-type waves, the portion of $(v_z \cdot B_x)$ with the sign of B_z changes from $\sim$ 3/4 (50% difference in Figure 5) in the years of the solar maximum to $\sim$ 9/11 (10% difference in Figure 5) during the solar minimum.

These Alfvén-type disturbances (propagating earthward) more effectively shift and displace the magnetospheric plasma sheet and break the magnetospheric configuration symmetry, which, in turn, may facilitate a substorm onset.

Based on our findings, we summarize the results in the following items.

1. The number of substorms, which started when the SW and IMF components product $(v_z \cdot B_x)$ had the same sign as the IMF B_z, was about twice larger than the number of substorms with the opposite signs of those at the time of an onset. This tendency was proved on two substorm onset lists, obtained by different methods.
2. The analysis of presubstorm changes in the number of periods with different signs of $(v_z \cdot B_x)$ shows that the number of periods with preferable sign (same as B_z at breakup) increases progressively during a growth phase and reaches its maximum in the last 5 min near the onset. This effect is especially notable for the substorms, which start under positive B_z, that means that not only B_z but also $(v_z \cdot B_x)$ changes its sign before an onset
3. Eleven-year statistics shows that similar imbalance exists in the SW. The product $(v_z \cdot B_x)$ has the same sign as B_z during 2/3 of all the time if we take the whole solar cycle period. This portion increases to 3/4 during the years near the solar maximum and decreases to 9/11 in years near the minimum of solar activity.

The last conclusion leads to a suggestion that the $(v_z \cdot B_x)$ value may be an important agent in substorm initiation, forcing an earlier breakup by changing plasma sheet motion direction. This suggestion needs further and more detailed (case) investigations of substorm dynamics.

Acknowledgments
We acknowledge the use of NASA/GSFC's Space Physics Data Facility (http://omniweb.gsfc.nasa.gov) for OMNI data. For the substorm data we gratefully acknowledge SuperMAG and Gjerloev, J. W. (Newell & Gjerloev, 2011) (http://supermag.jhuapl.edu/substorms/). This work was supported by Russian Foundation for Basic Research grants N 16-05-00470-a and 15-05-00879-a. The research of S. Dubyagin and N. Ganushkina leading to these results was partly funded by the European Union's Horizon 2020 research and innovation programme under grant agreement 637302 PROGRESS. The work of N. Ganushkina in Michigan was also partly supported by the National Aeronautics and Space Administration under grant agreements NNX14AF34G, NNX17AB87G and NNX17AI48G issued through the ROSES-2013 and ROSE-2016 programmes, respectively. The authors thank the Academy of Finland for the support of the Space Cooperation in the Science and Technology Commission between Finland and Russia (TT/AVA). We thank V. Sergeev for valuable comments and fruitful discussions.

References

Akasofu, S. I. (1975). Roles of north-south component of interplanetary magnetic-field on large-scale auroral dynamics observed by DMSP satellite. *Planetary and Space Science*, *23*, 1349–1354.

Belcher, J. W., & Davis, L. (1971). Large-amplitude Alfveń waves in the interplanetary medium, 2. *Journal of Geophysical Research*, *76*, 3534–3563.

Borovsky, J. E., & Yakymenko, K. (2017). Substorm occurrence rates, substorm recurrence times, and solar wind structure. *Journal of Geophysical Research: Space Physics*, *122*, 2973–2998. https://doi.org/10.1002/2016JA023625

Cowley, S. W. H. (1981). Asymmetry effects associated with the *x*-component of the IMF in a magnetically open magnetosphere. *Planetary and Space Science*, *29*(8), 809–818.

Dungey, J. W. (1961). Interplanetary magnetic field and the auroral zones. *Physical Review Letters*, *6*, 47–48.

Fairfield, D. H., & Cahill, J. L. J. (1966). Transition region magnetic field and polar magnetic disturbances. *Journal of Geophysical Research*, *71*(1), 155–169.

Freeman, M. P., & Morley, S. K. (2009). No evidence for externally triggered substorms based on superposed epoch analysis of IMF B_z. *Geophysical Research Letters*, *36*, L21101. https://doi.org/10.1029/2009GL040621

Frey, H. U., Mende, S. B., Angelopoulos, V., & Donovan, E. F. (2004). Substorm onset observations by IMAGE-FUV. *Journal of Geophysical Research*, *109*, A10304. https://doi.org/10.1029/2004JA010607

Gordeev, E. I., Sergeev, V. A., Amosova, M. V., & Andreeva, V. A. (2016). Influence of interplanetary magnetic field radial component on the position of the Earth's magnetotail neutral sheet. *Geophysical Methods of Survey the Earth and Its Subsoil*, 11–21. https://doi.org/10.13140/RG.2.1.4821.6565

Hoilijoki, S., Souza, V. M., Walsh, B. M., Janhunen, P., & Palmroth, M. (2014). Magnetopause reconnection and energy conversion as influenced by the dipole tilt and the IMF B_x. *Journal of Geophysical Research: Space Physics*, *119*, 4484–4494. https://doi.org/10.1002/2013JA019693

Kivelson, M. G., & Hughes, W. J. (1990). On the threshold for triggering substorms. *Planetary and Space Science*, *38*(2), 211–220.
Kubyshkina, M., Tsyganenko, N., Semenov, V., Kubyshkina, D., Partamies, N., & Gordeev, E. (2015). Further evidence for the role of magnetotail current shape in substorm initiation. *Earth, Planets and Space*, *67*, 139. https://doi.org/10.1186/s40623-015-0304-1
Lyons, L. R., Blanchard, G. T., Samson, J. C., Lepping, R. P., Yamamoto, T., & Morreto, T. (1997). Coordinated observations demonstrating external substorm triggering. *Journal of Geophysical Research*, *102*(A12), 27,039–27,051. https://doi.org/10.1029/97JA02639
Morley, S. K., & Freeman, M. P. (2007). On the association between northward turnings of the interplanetary magnetic field and substorm onsets. *Geophysical Research Letters*, *34*, L08104. https://doi.org/10.1029/2006GL028891
Newell, P. T., & Gjerloev J. W. (2011). Evaluation of SuperMAG auroral electrojet indices as indicators of substorms and auroral power. *Journal of Geophysical Research*, *116*, A12211. https://doi.org/10.1029/2011JA016779
Newell, P. T., Liou, K., Gjerloev, J. W., Sotirelis, T., Wing, S., & Mitchell, E. J. (2016). Substorm probabilities are best predicted romsolar wind speed. *Journal of Atmospheric and Solar-Terrestrial Physics*, *146*, 28–37. https://doi.org/10.1016/J.JASTP.2016.04.019
Panov, E. V., Nakamura, R., Baumjohann, W., Kubyshkina, M., Artemyev, A. V., Sergeev, V. A., et al. (2012). Kinetic ballooning/interchange instability in a bent plasma sheet. *Journal of Geophysical Research*, *117*, A06228. https://doi.org/10.1029/2011JA017496
Reistad, J. P., Östgaard, N., Laundal, K. M., Haaland, S., Tenfjord, P., Snekvik, K., et al. (2014). Intensity asymmetries in the dusk sector of the poleward auroral oval due to IMF B_x. *Journal of Geophysical Research: Space Physics*, *119*, 9497–9507. https://doi.org/10.1002/2014JA020216
Rostoker, G., & Falthammar, C. G. (1967). Relationship between changes in the interplanetary magnetic field and variations in the magnetic field at Earth's surface. *Journal of Geophysical Research*, *72*, 5853–5863.
Semenov, V. S., Kubyshkina, D. I., Kubyshkina, M. V., Kubyshkin, I. V., & Partamies, N. (2015). On the correlation between the fast solar wind flow changes and substorm occurrence. *Geophysical Research Letters*, *42*, 5117–5124. https://doi.org/10.1002/2015GL064806
Sergeev, V. A., Tsyganenko, N. A., & Angelopoulos, V. (2008). Dynamical response of the magnetotail to changes of the solar wind direction: An MHD modeling perspective. *Annals of Geophysics*, *26*, 2395–2402. https://doi.org/10.5194/angeo-26-2395-2008
Snekvik, K., Tanskanen, E. I., & Kilpua, E. K. J. (2013). An automated identification method for Alfvénic streams and their geoeffectiveness. *Journal of Geophysical Research: Space Physics*, *118*, 5986–5998. https://doi.org/10.1002/jgra.5058
Tanskanen, E. I. (2009). A comprehensive high-throughput analysis of substorms observed by IMAGE magnetometer network: Years 1993–2003 examined. *Journal of Geophysical Research*, *114*, A05204. https://doi.org/10.1029/2008JA013682
Tsyganenko, N. A., & Fairfield, D. H. (2004). Global shape of the magnetotail current sheet as derived from Geotail and Polar data. *Journal of Geophysical Research*, *109*, A03218. https://doi.org/10.1029/2003JA010062
Vörös, Z., Fasko, G., Khodanchenko, M., Honkonen, I., Janhunen, P., & Palmroth, M. (2014). Windsock memory Conditioned RAM (CO-RAM) pressure effect: Forced re- 313 connection in the Earth's magnetotail. *Journal of Geophysical Research: Space Physics*, *119*, 6273–6293. https://doi.org/10.1002/2014JA019857
Zhang, X.-Y., Moldwin, M. B., Steinberg, J. T., & Skoug, R. M. (2014). Alfvén waves as a possible source of long-duration, large-amplitude, and geoeffective southward IMF. *Journal of Geophysical Research: Space Physics*, *119*, 3259–3266. https://doi.org/10.1002/2013JA019623